# Three-dimensional structure of the wild-type RHDV

ZHENG Dong[1,4], XUE Tao[2], CHEN Donghua[1], ZHENG Ming[5], ZHOU Z. H.[2] & XU Wei[3]

1. Beijing Laboratory of Electron Microscopy, Institute of Physics, Chinese Academy of Sciences, Beijing 100080, China;
2. Department of Pathology and Laboratory Medicine, University of Texas-Houston Medical School, Houston, TX 77030, USA;
3. Institute of Biophysics, Chinese Academy of Sciences, Beijing 100101, China;
4. Analytical and Testing Center, Beijing Normal University, Beijing 100875, China;
5. China Institute of Veterinary Drug Control, Beijing 100081, China

Correspondence should be addressed to Xu Wei (e-mail: emlb@sun5.ibp.ac.cn)

Abstract **The three-dimensional (3D) structure of the wild-type rabbit hemorrhagic disease virus (RHDV) has been determined to a resolution of 3.2 nm by electron cryomicroscopy and computer image reconstruction techniques. The 3D density map exhibits characteristic structural features of a calicivirus: a *T*=3 icosahedral capsid with 90 arch-like capsomeres at the icosahedral and local 2-fold axes and 32 large surface hollows at the icosahedral 5- and 3-fold axes. This result confirms that the RHDV isolated in China is a member of the *Caliciviridae* family. A rather continuous capsid shell was found without channels. However, our RHDV structure also reveals some distinct structural characteristics not observed in other caliciviruses, including interconnected capsomeres and the lack of protuberance on the base of each of the surface hollows. Two types of particles were identified with similar outer capsid structure but different density distributions inside the capsid shells, which could not be distinguished by conventional negative staining electron microscopy. As the genomic and subgenomic RNAs are both packaged into particles for RHDV, we suggest that the two types of particles identified correspond to those containing either the genomic or subgenomic RNAs, respectively.**

**Keywords: electron cryomicroscopy, three-dimensional reconstruction, RHDV, calicivirus.**

Rabbit hemorrhagic disease virus (RHDV) was first described in 1984 in Jiangsu Province, China[1]. The virus causes a contagious disease in rabbits characterized by high morbidity and mortality. The typical pathological manifestation is hemorrhagic necrosis of the liver. Thus RHDV is an important pathogen affecting rabbit production.

The virus is non-enveloped, and its icosahedral capsid is 32—40 nm in diameter depending on various methods of negative staining electron microscopy. The viral genome consists of about 7.5 kb of positive sense single-stranded RNA, and has two open reading frames (ORF)[2]. ORF1, spanning about 86% of the whole genome, encodes for the major capsid protein of 60 ku (VP60), and several nonstructural proteins including p37 (helicase), a trypsin-like cysteine protein (TCP) and a putative RNA polymerase (pol)[3]. A minor capsid protein of 10 ku (VP10) is encoded by ORF2. After infection of cells, RHDV produces an additional RNA species of about 2.2 ku through transcription[4]. This subgenomic RNA encodes for the capsid proteins VP60 and VP10. Another structural protein VPg (virion protein, genome linked), encoded by ORF1, is convalently linked to 5′ ends of the genomic and subgenomic RNAs, respectively. Interestingly, the subgenomic RNA is packaged into the particle separately from the genomic RNA[5]. Up to now, RHDV has only been propagated in primary rabbit heptocytes[6]. The major capsid protein, VP60, has been expressed in the baculovirus system, which self-assembled into virus-like particle (VLP)[7]. Based on surface morphology and genome organization, RHDV has been assigned to the genus *Lagovirus* of *Caliciviridae*, which also includes the European Brown Hare Syndrome Virus (EBHSV)[8].

The three-dimensional structures have been determined for several caliciviruses including the recombinant Norwalk virus (rNV) capsid, a primate calicivirus and RHDV VLP[9—12]. However, no structural studies have been reported for the wild-type RHDV. Using electron cryomicroscopy and image reconstruction techniques, we determined the three-dimensional structure of the wild-type RHDV, establishing a framework for understanding its structure-function relationship and providing structural evidence for the classification of RHDV isolated in China.

## 1 Materials and methods

(ⅰ) Purification of RHDV. The RHDV strain 'Fuyang' was originally isolated in the Academy of Agricultural Science of Jiangsu Province, China. Researchers at the Institute of Husbandry and Veterinary Medicine there used the isolated virus to infect rabbit liver tissues, which were subsequently provided to us for virus purification.

Livers from infected rabbits were homogenized in PBS (pH 7.2, 1∶10 W/V). The homogenates were frozen and then thawed repeatedly for three times, and diluted in PBS (1∶2 V/V). After low speed centrifugation (8000 r/min, 40 min), the supernatant was precipitated with 6% polyethylenglycal 6000 (4℃, 12 h) and then centrifuged (8000 r/min, 40 min). The precipitate was resuspended in PBS. After the addition of the mixture of butanol and isopentanol (24∶1 V/V) and stirred for 5 min, the suspension was clarified by low speed centrifugation (2500 r/min, 30 min). The supernatant was collected and centrifuged (15000×*g*, 40 min). The supernatant was subjected to high speed centrifugation (145000×*g* for 2 h) (35 Ti rotor, Beckman). The pellets were resuspended in TNE (0.05 mol/L Tris, 0.05 mol/L NaCl, 0.005 mol/L EDTA),

layered on a cushion of 25% (W/V) sucrose solution in TNE and centrifuged at 145000×*g* (35 Ti rotor, Beckman) for 3 h. Then the pellets were resuspended in TNE for electron cryomicroscopy. The quality and concentration of RHDV were verified by negative staining electron microscopy.

(ii) Electron cryomicroscopy. Aliquots (~3 μL) of the virus suspension were applied to freshly carbon-coated holey EM grids, blotted with filter paper and then plunged into liquid ethane cooled by liquid nitrogen[13]. Specimens were transferred in a Philips CM12 operated at 100 kV and maintained at a temperature of about −170℃ in a Gatan 626 cryoholder. Images were recorded on Kodak SO163 film at a nominal magnification of 35000 times at about 1 and 2 μm underfocus, respectively, with an electron dose of about 1000 electrons/nm$^2$. In addition, images of large underfocus value (~5 μm) were recorded for analysis of mass density distribution at low spatial frequencies (low resolution).

(iii) Image processing and visualization. The micrographs without noticeable drift and charging were selected for digitization using a SCAI microdensitometer operated by a Windows NT PC (Zeiss). The scan step size was 14 μm/pixel, corresponding to 0.4 nm/pixel on the specimen scale. Subsequent image processing and visualization were performed on SGI workstations (Indigo2, and Octane with two CPUs) using custom designed software package[14]. The underfocus values of the micrographs were determined by the incoherent averaging of Fourier transforms of boxed out particle images[15]. The data of about 2 μm underfocus were used to calculate the initial center and orientation for each of virus particle images. For the refinement of center and orientation and final three-dimensional reconstruction, the data of about 1 μm underfocus were used. The orientation of virus particles was determined by Fourier common lines method[16]. The effective resolution was determined by the criterion of phase residual between two independent reconstructions less than 45°[17]. A total 361 virus particles were included for the three-dimensional reconstruction, which has an effective resolution of 3.2 nm.

## 2 Results

(i) Electron cryomicroscopic images. A typical area of a focal pair of electron cryomicrographs of the RHDV embedded in ice is shown in fig. 1. Due to the relatively large underfocus value of the far-from-focus micrograph in the focal pair, some characteristic capsomeres can be clearly seen protruding from the capsid surface (fig. 1(b)). Two types of particles can be observed in the micrograph according to their density differences inside the capsid shell: those with a high electron density and those with a very "light" electron density (hereafter referred to as the high- and low-density particles, respectively). The low-density particles are three times more abundant than the high-density particles. As can be seen in the 4.8 μm underfocus micrograph (fig. 1(b)), the densities inside the capsid shell for the low-density particle are concentrated in the core region, resulting in a gap between this core region and the capsid shell. For some low-density particles, this density core appears as a ring. However, the high- and low-density particles cannot be distinguished by negative staining electron microscopy (data not shown).

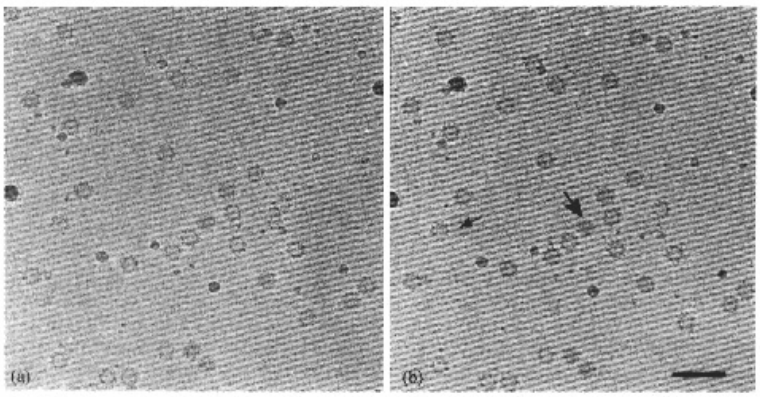


Fig. 1. Electron cryomicrographs of RHDV embedded in a thin layer of vitreous ice recorded at 2.2 (a) and 4.8 μm (b) underfocus. A high-density particle, and a low-density particle in (b) are indicated by a large and a small arrowheads, respectively. Bar = 100 nm.

(ii) Arch-like capsomeres and cup-shaped hollows. In the three-dimensional structure of RHDV (fig. 2), 90 arch-like capsomeres are arranged on a $T$ = 3 icosahedral lattice, forming a shell with 32 cup-shaped surface hollows. The arch-like capsomeres are located at the icosahedral and local 2-fold axes. The hollows, with the depth of 5 nm and the width of 8 nm, are located at the icosahedral 5- and 3-fold axes. The base (the bottom of the cup) of all the hollows is rather flat without noticeable surface protrusions.

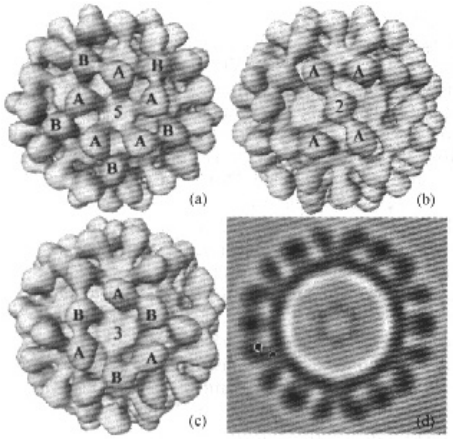


Fig. 2. Surface representations for the three-dimensional structure of RHDV viewed along the icosahedral 5- (a), 2- (b), and 3-fold (c) axes, and a central section perpendicular to the icosahedral 3-fold axis with the thickness of 0.4 nm (d).

Similar to other caliciviruses, the 90 capsomeres can be classified into two types: A and B. Type A capsomeres are located at the local 2-fold axes and there are five type A capsomeres surrounding each 5-fold axis. Located at the icosahedral 2-fold axes are type B capsomeres. Three type A and three type B capsomeres surround a 3-fold axis alternatively. Each type A capsomere is neighboring with two type B and two type A capsomeres (fig. 2(a)), whereas four type A capsomeres surround each type B capsomere (fig. 2(b)). Therefore, the two types of capsomeres are situated in different local environments.

(iii) Inter-connections between type A and B capsomeres. The capsomeres are inter-connected by a density band at the diagonally opposite corners of the platform of the type B capsomere (fig. 2). A type B capsomere is linked to two neighboring type A capsomeres, whereas each type A capsomere is connected only to one type B capsomere. Several independent reconstructions show similar interconnections between the capsomeres (data not shown).

(iv) The continuity of capsid shell. The central slice (0.4 nm thick) perpendicular to the 3-fold axis of the three-dimensional map shows that the inner and outer radii are about 11.7 and 15.2 nm for the capsid shell, respectively (fig. 2(d)). The capsid shell has a thickness of 3.5 nm. At the current resolution, the mass densities of the shell are rather continuous and do not reveal any channels or holes.

(v) Radial density plot. The averaged mass density distributions as a function of radius for the high- and low-density particles are shown in fig. 3. The mass density distribution can be divided into three regions, designated as C, S and P, corresponding to radial regions between 0—10.0, 11.7—15.2, and 15.2—20.0 nm, respectively. These regions represent the density core (C), the capsid shell (S), and the protruding portion of the capsomere (P) of the capsid. The most significant differences in density distributions of the high- and low-density particles are observed in the region C. The negative peak at the radius of 21.6 nm represents the boundary of the virus particle, which results from the Fresnel effect of the contrast transfer function (CTF) of the electron microscope.

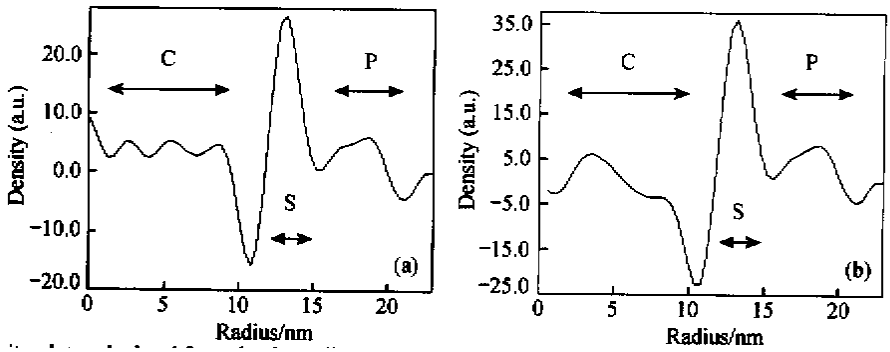


Fig. 3. Radial density plots calculated from the three-dimensional density map for the high-density particle (a), and the low-density particle (b) of RHDV. The letters C, S, and P indicate the core, the shell, and the protruding capsomere of the virus, respectively.

## 3 Discussion

(i) The capsid structure. The high- and low-density particles of RHDV exhibit characteristic structural features of caliciviruses, such as 90 arch-like capsomeres and 32 cup-shaped hollows arranged on a $T = 3$ icosahedral capsid. These structural features have also been seen in the rNV capsid, the primate calicivirus and the RHDV VLP[9—12]. However, our RHDV structure also showed

several unique structural features not observed in other caliciviruses. First, the arch-like A and B type capsomeres are interconnected at their upper domains, in addition to their shell domains. The upper inter-capsomere connections were not observed in the rNV capsid and primate calicivirus reconstructions[9—11]. It should be pointed out that the capsomeres in a low resolution structure of the RHDV VLP were also linked on the bottom by a density bulging from the capsid shell for the RHDV VLP[12]. This observation is different from that of the inter-capsomere connection seen in our wild-type RHDV structure. Thus, higher resolution structures are needed to verify the differences in the inter-capsomere connections between wild-type particles and VLPs of RHDV. Second, the base of each of cup-shaped hollows is rather flat in RHDV regardless of its location, whereas there is protuberance on the base located at both 5- and 3-fold axes in the rNV capsid, the primate calicivirus, and the RHDV VLP.

Amino acid sequence analysis revealed that the variable portion of the capsid protein VP60 sequence is located at the central region of the sequence among caliciviruses, while the N-terminal region is highly conserved[18]. This analysis suggests that the variable portion of the major capsid protein sequence is located at the surface of the virion and the conserved portion is located at the interior of the virion. The X-ray structure confirmed that the N-terminal 225 residues constitute the capsid shell for the rNV capsid[9]. The difference in the inter-cap- somere connections between RHDV and other calicivi- ruses correlated well with the variable portion of the VP60 sequence.

In addition, the secondary structure prediction has indicated that the capsid protein VP60 folds into predominant β-fold structure (data not shown). The capsid shell domain of the rNV capsid protein has an eight- stranded, sandwich structure[9]. The dimensions of the capsid shell of the rNV and RHDV are also similar. Therefore, it is conceivable that for RHDV the major capsid protein VP60 may also fold into the sandwich structure in the capsid shell.

(ii) Identification of the viral particles containing the subgenomic RNA. In the electron cryomicroscopy images of RHDV (fig. 1), the high- and low-density particles are clearly seen. However, these two types of particles cannot be distinguished by negative staining electron microscopy (data not shown). Nearly all RHDV particles appear as 'full'. It was reported that the negative stains could not penetrate the capsid shell of the RHDV VLP[12]. Thus the low-density particles cannot be discerned from the high-density particles for RHDV by negative staining electron microscopy.

On the basis detailed below, we suggest that the high- and low-density particles observed in our image represent the RHDV particles containing the genomic and subgenomic RNA, respectively. First, RHDV produces the subgenomic RNA after infection of cells, encoding for capsid proteins VP60 and VP10, and this RNA species is packaged into the viral particles. Sucrose density gradient centrifugation and hybridization indicated that the subgenomic RNA is packaged into the viral particle separately from the genomic RNA[5]. The difference between the genomic and subgenomic RNA is more than 5 kb and it is very likely to distinguish the two particle species with electron cryomicroscopy. Second, the only difference between the high- and low-density particles is the density distributions inside the capsid shell (fig. 1). Some of the low-density particles have a ring-shaped density core inside the capsid shell and a prominent gap between the density core and the capsid shell. This accords well with the averaged radial density distributions of the reconstruction of the low-density particles (fig. 3(b)). The plot demonstrates that the density inside the capsid shell constitutes a concentric shell and a gap exists partitioning this density shell and the capsid shell. In contrast, the radial density plot of RHDV VLPs showed that the mass density inside the capsid shell is lower than the ice background[12]. Finally, at the present resolution, no channels or holes are seen on the capsid shell of the RHDV particles. Moreover, the atomic resolution structure of rNV did not reveal holes with an appropriate size used for viral RNA encapsidation and release. Thus it is unlikely that the low-density particles are caused due to the release of the genomic RNA.

A common feature possessed by caliciviruses is that they have subgenomic RNAs. However, it has been found that only the subgenomic RNA of RHDV is separately packaged into particles from the genomic RNA[7]. Further biochemical and structural studies will elucidate the significance of such packaging.

(iii) Classification of RHDV isolated in China. It had long been controversial about whether the genome is ssDNA or ssRNA for RHDV of China origin as well as its classification. Nucleic acid hybridization showed that the genome of RHDV isolated in China is homologous with the cDNA from RHDV of German origin[19]. Thus, as RHDV of German strain, the virus from China should also be a member of the *Caliciviridae* family. The 3D structure of RHDV presented here showed characteristic features common to caliciviruses. Therefore, our three-dimensional structure of RHDV provides a solid structural evidence that RHDV is a member of the *Caliciviridae*.

**Acknowledgements** Liver tissue of rabbits died of typical RHD was kindly provided by Prof. Dong Yafang at the Institute of Husbandry and Veterinary affiliated to the Academy of Agricultural Sciences of Jiangsu Province, China. Prof. K. H. Kuo at Beijing Laboratory of Electron Microscopy, Chinese Academy of Sciences, has encouraged and supported the authors. This work was supported by the National Natural Science Foundation of China (Grant Nos. 69501008 and 19634020). Research in Houston has been supported by NIH (AI 46420) and the Welch Foundation (AU-1492).

## References


1. Liu, S. J., Xue, H. P., Pu, B. Q. et al., A new viral disease in rabbits, Anim. Husb. Vet. Med. (in Chinese), 1984, 16(6): 253.
2. Meyers, G., Wirb1ich, C., Thie1, H-T., Rabbit hemorrhagic disease virus-molecular cloning and nucleotide sequencing of a calicivirus genome, Virol., 1991, 184(2): 664.
3. Wirblich, C., Thiel, H.-J., Meyers, G., Genetic map of the calicivirus rabbit hemorrhagic disease virus as deduced from *in vitro* translation studies, J. Virol., 1996, 70(11): 7974.
4. Cubitt, D., Bradley, D. W., Carter, M. J. et al., *Ca1iciviridae*, in Virus Taxonomy, (eds. Murphy, F. A., Fauquet, C. M., Bishshop, D. H. L. et al.), 6th Rep. Int. Committee on Taxonomy of Viruses, New York: Springer, 1995, 359—363.
5. Meyers, G., Wirb1ich, C., Thiel, H-T., Genomic and subgenomic RNAs of rabbit hemorrhagic disease virus are both protein-linked and packaged into particles, Virol., 1991, 184(2): 677.
6. König, M., Thiel, H.-J., Meyers, G., Detection of viral proteins after infection of cultured hepatocytes with rabbit hemorrhagic disease virus, J. Virol., 1998, 72(5): 4492.
7. Thie1, H.-T., König, M., Calicivirus: An overview, Vet. Microbiol., 1999, 69(1—2): 55.
8. Laurent, S., Vautherot, J. F., Madelaine, M. F. et al., Recombinant rabbit hemorrhagic disease virus capsid protein expressed in baculovirus self-assembles into virus like particles and induces protection, J. Virol., 1994, 68(10): 6794.
9. Prasad, B. V. V., Hardy, M. E., Docland, T. et al., X-ray crystallographic structure of the Norwalk virus capsid, Science, 1999, 286(5438): 287.
10. Prasad, B. V. V., Rothnagel, R., Jiang X. et al., Three-dimensional structure of baculovirus-expressed Norwalk virus capsids, J. Virol., 1994, 68(8): 5117.
11. Prasad, B. V. V., Matson, D. O., Smith, A. W., Three-dimensional structure of calicivirus, J. Mol. Biol., 1994, 240(3): 256.
12. Thouvenin, E., Laurent, S., Madelaine, M. F. et al., Bivalent binding of a neutralising antibody to a calicivirus involves the torsional flexibility of the antibody hinge, J. Mol. Biol., 1997, 270(2): 238.
13. Dubochet, J., Adrian, M., Chang, J.-J. et al., Cryo-electron microscopy of vitrified specimens, Quart. Rev. of Biophy., 1988, 21: 129.
14. Zhou, Z. H., Chiu, W., Haskell, K. et al., Refinement of herpesvirus B-capsid structure on parallel supercomputers, Biophy. J., 1998, 74(1): 576.
15. Zhou, Z. H., Hardt, S., Wang, B. et al., CTF determination of images of ice-embedded single particles using a graphics interface, J. Struct. Biol., 1996, 116(1): 216.
16. Crowther, R. A., Procedures for three-dimensional reconstruction of spherical viruses by Fourier synthesis from electron micrographs, Phil. Trans. Roy. Soc. Lond, B, 1971, 261: 221.
17. Zhou, Z. H., Prasad, B. V. V., Jakana, J. et al., Protein subunit structures in the herpes simplex virus A-capsid determined from 400 kV spot scan electron cryomicroscopy, J. Mol. Biol., 1994, 242(4): 456.
18. Wirblich, C., Meyers, G., Ohlinger, V. F. et al., European brown hare syndrome virus: Relationship to rabbit hemorrhagic disease virus and other calicivirus, J. Virol., 1994, 68(8): 5164.
19. Cui, Z. Z., Duan, Y. Y., Wang, Y. K. et al., Comparison of genomes of Chinese and German strains of rabbit haemorrhagic disease virus, Chinese J. of Virol. (in Chinese), 1995, 11(3): 242.


(Received December 4, 2000)